

Effects of platelet-rich plasma on mesenchymal stem cells isolated from rat uterus

Polina Vishnyakova^{Corresp., Equal first author, 1, 2}, Daria Artemova^{Equal first author, 1}, Andrey Elchaninov^{1, 3}, Zulfiia Efendieva⁴, Inna Apolikhina^{1, 4}, Gennady Sukhikh¹, Timur Fatkhudinov^{2, 5}

¹ National Medical Research Center for Obstetrics, Gynecology and Perinatology Named after Academician V.I. Kulakov of Ministry of Healthcare of Russian Federation, Moscow, Russia

² People's Friendship University of Russia, Moscow, Russia

³ Pirogov Russian National Research Medical University (RNRMU), Moscow, Russia

⁴ I. M. Sechenov First Moscow State Medical University of Ministry of Health of Russia (Sechenov University), Moscow, Russia

⁵ Scientific Research Institute of Human Morphology, Moscow, Russia

Corresponding Author: Polina Vishnyakova
Email address: vpa2002@mail.ru

Background. Platelet-rich plasma (PRP) is a valuable source of growth factors widely used in regenerative medicine. Recently, PRP was used for to treat infertility caused by refractory thin endometrium. Mesenchymal stem/stromal cells (MSCs) of endometrium are an essential cellular component responsible for extracellular matrix remodeling, angiogenesis, cell-to-cell communication, post-menstrual tissue repair etc. We examined the effects of PRP on the MSCs isolated from rat uterus and compared them with the effects of ordinary plasma (OP).

Methods. MSCs were isolated from rat uterus by enzymatic disaggregation. Flow cytometry analysis was used for the immunophenotyping of the primary cells. The ability of MSCs to differentiate in osteo-, chondro- and adipogenic directions was assessed with differentiation-induced media. Immunocytochemistry assay was performed for Ki-67 and vimentin staining. Autophagy and apoptosis markers as well as the level of MMP9 and ER α was assessed by western blotting.

Results. After 24 h incubation of MSCs proliferation index was significantly higher for PRP compared to OP and complete growth medium. The treatment with PRP and OP enhances activation of autophagy while OP also induced up-regulation of stress-induced protein p53 and extracellular enzyme MMP9. Significantly elevated level of MMP9 production was observed in both OP group compared to complete growth medium and PRP. These results indicate the practical relevance and validity of PRP usage in treatment of infertility.

1 Effects of platelet-rich plasma on mesenchymal stem 2 cells isolated from rat uterus

3

4 Vishnyakova Polina ^{1,2#*}, Artemova Daria ^{1#}, Elchaninov Andrey ^{1,3}, Efendieva Zulfia⁴,
5 Apolikhina Inna ^{1,4}, Sukhikh Gennady ¹ and Fatkhudinov Timur ^{2,5}

6 Author affiliations:

7 ¹ National Medical Research Center for Obstetrics, Gynecology and Perinatology Named after
8 Academician V.I. Kulakov of Ministry of Healthcare of Russian Federation, Moscow, Russia

9 ² Peoples' Friendship University of Russia, Moscow, Russia

10 ³ Pirogov Russian National Research Medical University (RNRMU)

11 ⁴ Institute of Professional Education of the I. M. Sechenov First Moscow State Medical
12 University of Ministry of Health of Russia (Sechenov University)

13 ⁵ Scientific Research Institute of Human Morphology, Moscow, Russia

14 # – equal contribution

15

16 Corresponding Author:

17 Polina A. Vishnyakova, PhD

18 Laboratory of regenerative medicine, Research Center for Obstetrics, Gynecology and
19 Perinatology, Ministry of Healthcare of the Russian Federation, 4, Oparina street, Moscow,
20 17513, Russia. Tel: +79150658577.

21 Email: vpa2002@mail.ru or vishnyakovapolina@gmail.com

22

23 Abstract

24

25 **Background.** Platelet-rich plasma (PRP) is a valuable source of growth factors widely used in
26 regenerative medicine. Recently, PRP was used for to treat infertility caused by refractory thin
27 endometrium. Mesenchymal stem/stromal cells (MSCs) of endometrium are an essential cellular
28 component responsible for extracellular matrix remodeling, angiogenesis, cell-to-cell
29 communication, post-menstrual tissue repair etc. We examined the effects of PRP on the MSCs
30 isolated from rat uterus and compared them with the effects of ordinary plasma (OP).

31 **Methods.** MSCs were isolated from rat uterus by enzymatic disaggregation. Flow cytometry
32 analysis was used for the immunophenotyping of the primary cells. The ability of MSCs to
33 differentiate in osteo-, chondro- and adipogenic directions was assessed with differentiation-

34 induced media. Immunocytochemistry assay was performed for Ki-67 and vimentin staining.
35 Autophagy and apoptosis markers as well as the level of MMP9 and ER α was assessed by
36 western blotting.

37 **Results.** After 24 h incubation of MSCs proliferation index was significantly higher for PRP
38 compared to OP and complete growth medium. The treatment with PRP and OP enhances
39 activation of autophagy while OP also induced up-regulation of stress-induced protein p53 and
40 extracellular enzyme MMP9. Significantly elevated level of MMP9 production was observed in
41 both OP group compared to complete growth medium and PRP. These results indicate the
42 practical relevance and validity of PRP usage in treatment of infertility.

43

44 **Introduction**

45

46 Platelet-rich plasma (PRP) is plasma with a platelet concentration above normal (Theoret &
47 Stashak, 2014) The increased platelet counts in PRP deliver increased amounts of the growth
48 factors enclosed within the platelet granules, including platelet-derived growth factors (PDGF:
49 PDGF-AA, PDGF-BB, and PDGF-AB), transforming growth factors (TGF), insulin-like growth
50 factors (IGF), vascular endothelial growth factor (VEGF), epidermal growth factor (EGF),
51 connective tissue growth factor (CTGF), fibroblast growth factors (FGF) (Lubkowska,
52 Dolegowska & Banfi, 2012) etc. PRP is also rich in certain plasma proteins e.g. fibrin,
53 fibronectin and vitronectin (Marx, 2019). For the platelet degranulation and fibrinogen cleavage,
54 plasma samples are usually activated by the addition of calcium chloride (alternatively, thrombin
55 or collagen) or by applying freeze/thaw cycle(s) (Cavallo et al., 2016; Maffulli, 2016). The view
56 of PRP as a potential therapeutic agent for tissue regeneration was initiated by Marx et al. (Marx
57 et al., 1998). In 1998, these authors found that the addition of PRP to a bone graft during the
58 bone-milling phase of its preparation enhanced the rates of bone formation in the treatment of

59 human mandibular defects. Nowadays, PRP is widely used in cosmetology, dentistry, sports
60 medicine and surgery (Yuksel et al., 2014; Maffulli, 2016; Patel et al., 2016). PRP could be
61 applied to the site of injury, mixed with a bone graft, layered over the graft upon its placement in
62 the body, sprayed onto the surface of tissue, applied over the graft or used as a biological
63 membrane (Civinini et al., 2011). In a recent study by Kim et al., intrauterine administration of
64 the autologous PRP improved the implantation and pregnancy outcomes for the patients with
65 refractory thin endometrium resulting in ≥ 2 failed *in vitro* fertilization cycles (Kim et al., 2019).
66 These results are encouraging: they indicate that the PRP effects on the refractory thin
67 endometrium may have a potential for the assisted reproductive technology. Endometrium is a
68 dynamic structure composed of simple columnar epithelium with uterine glands, and the
69 underlying stroma (Pertschuk, 1990) with blood vessels, nerves, collagen and reticular fibers,
70 and a variety of stromal cells (Aplin, 2018). Isolation of mesenchymal stem/stromal cells
71 (MSCs) from endometrium (Chan, Schwab & Gargett, 2004; Chan & Gargett, 2006) allows
72 elucidation of tissue-specific functions and markers of these cells thus opening new prospects of
73 their usage. As actively proliferating cells, MSCs play an important role in the tissue homeostasis
74 of endometrium — they are involved in the extracellular matrix remodeling, angiogenesis, cell-
75 to-cell communication, post-menstrual tissue repair, etc.(Mutlu, Hufnagel & Taylor, 2015;
76 Arutyunyan et al., 2016) The use of rat endometrial MSCs makes a good model for studying the
77 action of PRP in the perspective of infertility treatment. Despite the expanding use of PRP in
78 clinical practice, exact molecular mechanisms of the PRP action on cells are largely unclear. In
79 current study, we examine the effects of PRP on the MSCs isolated from rat uterus. We compare
80 them with the effects of ordinary plasma (OP).

81 **Materials & Methods**

82

83 Ethical disclosure

84 The authors state that they have obtained appropriate institutional review board approval or have
85 followed the principles outlined in the Declaration of Helsinki for all human or animal
86 experimental investigations. The study was approved by the Ethical Review Board at the
87 Scientific Research Institute of Human Morphology (Protocol №.15, 9th of December, 2019).
88 **Animals.** The outbred eight-week-old female Sprague-Dawley rats of 250–300 g weight were
89 obtained from the Institute for Bioorganic Chemistry branch animal facilities (Pushchino,
90 Moscow region, Russia). All experimental work involving animals was carried out according to
91 the standards of laboratory practice (National Guidelines No. 267 by Ministry of Healthcare of
92 the Russian Federation, June 1, 2003), and all efforts were made to minimize the suffering. The
93 study was approved by the Ethical Review Board at the Scientific Research Institute of Human
94 Morphology (Protocol №.15, 9th of December, 2019). The animals were adapted to the
95 laboratory conditions (23°C, 12 h/12 h light/dark, 50% humidity, and ad libitum access to food
96 and water) for 2 weeks prior to the experiments. In adult female rats, the stage of the estrous
97 cycle was determined by taking a vaginal smear. The smear was stained with methylene blue and
98 the stage was determined by assessment of cellular composition of the smear. The uterus was
99 dissected at the stage of metestrus after euthanasia in CO₂-chamber; the blood was collected by
100 puncture from the heart. Animals served only as a source of the uterus and autologous plasma;
101 therefore, no experimental conditions and endpoints were used.

102 **PRP and OP preparation.** The blood was collected in tubes with 2 ml of heparin (5000 IU/ml)
103 and 800 µl of 10% sodium citrate. PRP was obtained based on a protocol developed by Yazigi et
104 al. (Yazigi Junior et al., 2015) The blood was centrifuged at 400 g for 10 min, the plasma was
105 collected in a new tube and centrifuged again at 4 °C, 400 g for 10 min. After centrifugation,

106 70% of the supernatant (the platelet-poor plasma, PPP) was discarded. The remaining fraction
107 PRP, which according to the modern classification belongs to L type (L-PRP), was preserved.
108 The platelet counts were determined on a TC20 Automated Cell Counter (Bio-Rad, USA) and
109 constituted 50×10^6 platelets/ml on average. To obtain OP, the blood was centrifuged at 4 °C,
110 2000 g for 15 min, and the supernatant was collected. The prepared OP and PRP were aliquoted,
111 frozen and stored at -20 °C. Before use, PRP was activated by adding 10% CaCl₂ (10 µl of per
112 200 µl of PRP) according to the protocol by Messori et al.(Messori et al., 2011)

113 ***The protocol for obtaining MSCs from rat endometrium.*** The primary cell cultures were
114 obtained based on the protocol by De Clercq et al. with modifications (De Clercq, Hennes &
115 Vriens, 2017). The dissected uterus was minced with scissors in Hank's Balanced Salt Solution
116 (HBBS) and transferred into 0.25% trypsin. The tube was incubated at 4 °C for 1 h, then at 22 °C
117 for 1 h, and finally at 37 °C for 15 min with periodical shaking. The supernatant was taken and
118 the solid bulk was transferred to a solution of collagenases type I and type IV in 0.05% trypsin-
119 EDTA solution (collagenase I:collagenase IV:trypsin-EDTA, 1:1:10), incubated at 37 °C for 30
120 min, and passed through a 70 µm cell strainer. The material remaining on the strainer was
121 transferred to a fresh solution of collagenases with 0.05% trypsin-EDTA, incubated at 37 °C for
122 15 min, and passed through a strainer again. The resulting suspension containing the cells of
123 interest was centrifuged at 300 g for 5 min at 22 °C. The pellet was resuspended in HBBS
124 supplemented with 1% FBS, centrifuged again, and resuspended in complete growth medium
125 (DMEM/F-12 supplemented with 10% FBS, L-glutamine and penicillin/streptomycin) for
126 cultivation. The obtained cells were verified for compliance with the minimal criteria for MSCs
127 issued by the International Society for Cellular Therapy(Dominici et al., 2006) (adhesion to
128 untreated plastic, specific profile of surface antigens, and *in vitro* differentiation towards

129 osteogenic, chondrogenic and adipogenic progeny). To assess the effects of PRP and OP on
130 MSCs, the cells were cultured for 24 h in the medium supplemented with 10% PRP and 10% OP,
131 respectively, instead of FBS. CGM with 10% FBS was used as the control.

132 **Flow cytometry analysis.** Immunophenotyping of the cells for the surface and intracellular
133 markers was performed upon reaching 80% confluence. The harvested cells were centrifuged at
134 800 g for 10 min, the supernatant was discarded, the cells were fixed in 2% paraformaldehyde
135 for 15 min at room temperature (RT), diluted with 5 ml of PBS, and centrifuged at 1500 g for 10
136 min. The pellet was resuspended in 1 ml of PBS. For immunostaining, 1×10^5 of fixed cells
137 were incubated in 100 μ l of Rinsing Solution (Miltenyi Biotec, USA) with primary antibodies to
138 CD90 (ab225, 1/100, Abcam), CD45 (130-107-846, clone REA504, 1/20, Miltenyi Biotec),
139 CD105 (ab107595, 1/100, Abcam), CD34 (PAB18289, 1/100, Abnova) at room temperature for
140 1 h, and subsequently with secondary antibodies — anti-mouse Ig-FITC (ab6785, 1/500, Abcam)
141 or anti-rabbit Ig-PE (sc-3739, 1/100, Santa Cruz) at RT for 1 h in the dark. After the incubation,
142 the cells were washed in PBS, resuspended in 0.5 ml of PBS, and transferred to fresh tubes for
143 the analysis on a FACScan flow cytometer (Becton Dickinson, USA) with the CellQuest
144 software.

145 **Induced differentiation of MSCs.** The ability of MSCs to differentiate in osteo-, chondro- and
146 adipogenic directions was assessed at early passages (up to 7). The cells were grown to 70%
147 confluency in CGM, and then the growth medium was replaced with differentiation medium (for
148 differentiation) or CGM (for the controls). Differentiation into adipogenic progeny was
149 accomplished by using StemPro® Adipogenesis Differentiation Kit (Gibco) in the course of 7
150 days. At the end of the differentiation process, the cells were fixed with ethyl alcohol:formalin
151 solution (1:4) for 3 minutes and stained with Sudan III (5.7 mM) for 10 minutes to visualize fat

152 droplets. For osteogenic differentiation, the medium was supplemented with dexamethasone (10⁻⁷ M) and ascorbic acid (0.2 mM) in the course of two weeks. At the end, the cells were fixed
153 with 70% alcohol, and for the detection of mineralization sites, the cells were stained with 40
154 mM alizarin red S solution (pH = 4.7) for 5 min. Chondrogenic differentiation was performed by
155 using StemPro® Chondrogenesis Differentiation Kit (Gibco). After two weeks of differentiation,
156 the cells were fixed with 4% formalin for 1 h and for detection of mucopolysaccharides were
157 stained with 1% alcian blue for 24 h. Samples were analyzed using an Axiovert 40 CFL inverted
158 microscope (Zeiss, Germany) using ZEN software (Carl Zeiss, Germany).

160 **Immunocytochemistry.** The MSCs were grown on glass coverslips (Fisher Scientific) coated
161 with gelatin and placed in Petri dishes (35 × 10 mm). For immunocytochemistry, the cells were
162 fixed in 2% paraformaldehyde. The coverslips with fixed cells were treated with 0.1% Triton X-
163 100 for 10 min (cell membrane permeabilization) and washed with PBS. Non-specific binding
164 sites were blocked with 1% BSA in PBS with 0.1% Tween-20 for 30 minutes. The coverslips
165 were incubated with antibodies to Ki-67 (ab15580, 1/100, Abcam) or vimentin (ab8978, 1/250,
166 Abcam) at +4 °C for 24 hours. After incubation, the coverslips were washed with PBS and then
167 incubated with the secondary anti-rabbit-PE antibodies (1/200) or anti-rabbit-FITC antibodies
168 (1/200) in the dark at RT for 1 h and subsequently washed with PBS. To stain the nuclei, the
169 coverslips were incubated with DAPI (0.004 mg / ml) at 37 °C for 10 min. Then the coverslips
170 were washed in PBS and mounted in Aqua-Poly Mount. The photographs were made using a
171 Leica DM 4000B fluorescence microscope (Leica Microsystems, Germany) with the LAS AF
172 v.3.1.0 software (Leica Microsystems, Germany).

173 **Western blot assay.** The cells were washed with PBS and lysed in the ice-cold RIPA buffer. The
174 sample was mixed with 2X loading buffer and incubated at 95 °C for 1 minute. The samples

175 were stored at -80 °C until use and heated for 1 min at 95 °C before loading. The proteins were
176 separated by 10–12.5% sodium dodecyl sulfate polyacrylamide gel electrophoresis (SDS-PAGE)
177 and transferred from the gel to PVDF membranes by the semi-wet approach using Trans-Blot®
178 Turbo™ RTA Mini LF PVDF TransferKit (Bio-Rad Laboratories, Inc.). The membranes were
179 blocked with 5% milk in Tris-buffered saline containing 0.1% Tween (TTBS) at RT for 1 h, then
180 stained overnight with primary antibodies to LC3B (ab48394, Abcam), Bcl-2 (ab32124, Abcam),
181 p53 (ab90363, Abcam), ER α (ab3575, Abcam), MMP-9 (ab38898, Abcam) and GAPDH (sc-
182 25778, Santa Cruz) and subsequently with the HRP-conjugated secondary antibodies (Bio-Rad
183 Laboratories, Inc.). Chemiluminescent signal developed by using Novex ECL Kit (Invitrogen,
184 USA) was visualized in a C-DiGit® Blot Scanner (LI-COR, USA) using the Image Studio™
185 Acquisition Software (LI-COR, USA). Figure of uncropped membrane is available in
186 Supplementary information (Fig.S1). The relative protein levels were determined via
187 normalization by GAPDH signals.

188 **Statistical analysis.** Statistical data processing was performed in the GraphPad Prism 8
189 (Software GraphPad Software, USA). The normality of distributions was tested by the Shapiro-
190 Wilk criterion. In the case of normal distribution, one-way ANOVA with the Turkey post-hoc
191 test for multiple comparison was used. In the case of non-normal distribution, the Kruskal-Wallis
192 test with the post-hoc Dunn test was used. The differences were considered statistically
193 significant at $p < 0.05$.

194 **Results**

195

196 **Characterization of isolated MSCs.** The uterus is a non-classical source of MSCs. Given the
197 wide variability of MSC phenotypes and tissue-specific features (Kwon et al., 2016) the first
198 stage of our study was to show the compliance of rat uterine mesenchymal cell cultures to the

199 established minimal criteria for MSCs, including phenotype profile and the capability of induced
200 *in vitro* differentiation into different mesenchymal lineages. The obtained cultures of fibroblast-
201 like cells were immunophenotyped by flow cytometry for CD90, CD105, CD45 and CD34. The
202 region of interest was selected by relation of forward and side scattering values in a FSC-SSC
203 dot plot diagram (Figure 1 b), reflecting the size and granularity of the cells, respectively. We
204 gated the major pool of single cell events (R1) excluding debris (Figure 1 a). The peaks of
205 fluorescence were distinctly shifted in histograms for the MSC samples stained specifically with
206 antibodies to CD90 and CD105 compared with the controls stained with secondary antibodies
207 only (green curve). We found that 72.7% of the cells were positive for CD90 and 31.8% of the
208 cells were positive for CD105, which indicated correspondence of the obtained cultures to the
209 CD90+CD105+ phenotype. Interestingly, 3.1% and 20.1% of the cells were positive for CD45
210 and CD34, respectively. To further confirm the compliance, we stained the cultures for vimentin.
211 The immunocytochemical assay revealed the presence of vimentin protein in 100% of the cells
212 (Figure 1 b).

213 We promoted differentiation of the cell cultures into adipogenic, osteogenic and chondrogenic
214 lineages by using specific combinations of inducers. The adipogenic differentiation was
215 identified by formation of lipid droplets revealed by staining with Sudan III (Figure 1 c). During
216 the osteogenic differentiation, the cells formed characteristic conglomerates, with the foci of
217 calcification revealed by alizarin red staining (Figure 1 c). During the chondrogenic
218 differentiation, conglomerates were also formed by the cells, and the mucopolysaccharide
219 production was revealed by staining with alcian blue (Figure 1 c).

220 **Effects of PRP and OP on cell proliferation and cell death.** Effects of PRP and OP on the rat
221 uterine MSC cultures were evaluated after 24 h incubation of the cells in a medium containing

222 10% PRP or 10% OP instead of FBS. Accordingly, complete growth medium (CGM) with 10%
223 FBS was used as the control. Proliferation was assessed by immunocytochemical staining for Ki-
224 67 following the incubation (Figure 2 a). The percentage of Ki-67 positive nuclei divided by the
225 total number of nuclei (proliferation index) was 18.1% for CGM, 41.9% for PRP, and 21.7% for
226 OP (Fig. 2 b). For PRP, the differences were statistically significant ($p = 0.04$).

227 To evaluate the activation or inhibition of apoptosis, we analyzed the production of the stress-
228 induced protein p53 and the anti-apoptotic protein Bcl-2. The p53 protein levels were
229 significantly higher in the cells exposed to OP ($p = 0.03$), as compared with the control (CGM)
230 cells (Figure 2 c). Relative levels of Bcl-2 production did not differ among the studied groups.
231 Autophagy was assessed by the level of production of the autophagy marker LC3B. Western blot
232 analysis revealed elevated production of LC3B protein in the cells exposed to PRP or OP, as
233 compared with the control (CGM, Figure 2 c); the observed effect was statistically significant
234 among studied groups.

235 **Endometrium receptivity: effects of PRP and OP on the matrix metalloproteinase 9**

236 **(MMP9) and estrogen receptor α (ER α) production.** Zinc-metalloproteinase MMP9

237 participates in the extracellular matrix remodeling. We estimated potential invasiveness of MSCs
238 as a correlate of MMP9 production. Although elevated levels of MMP9 production were
239 observed in both OP and PRP groups compared to CGM, only in the OP treated cultures the
240 MMP9 upregulation was significant (Figure 3) ($p=0.03$). In addition, we compared the levels of
241 ER α , which can be partially associated with endometrial receptivity. Despite the elevated ER α
242 levels in the PRP and OP treated cultures, the difference was not significant.

243 **Discussion**

244 Administration of PRP for the treatment of thin endometrium has been already introduced to

245 clinical practice in a pilot study by Kim et al. aimed at increasing the endometrium thickness and
246 accordingly the probability of implantation (Kim et al., 2019). However, the mechanism of the
247 positive effect of PRP on the endometrium thickness remains uncertain. In this study, we attempt
248 to identify signaling pathways activated in the multipotent stromal cells of endometrium under
249 the influence of PRP by using rat endometrium as a model. Endometrial MSCs play a key role in
250 the stroma: they participate in the regeneration of the functional layer of the endometrium due to
251 the presence of receptors for sex hormones and the ability for extracellular matrix remodelling
252 (Mutlu, Hufnagel & Taylor, 2015). These features emphasize the importance of MSCs for
253 receptivity of the endometrium during the implantation period. We isolate primary cultures of
254 stromal cells from the rat uterus and prove that these cells are essentially MSCs by their ability to
255 differentiate in adipogenic, osteogenic and chondrogenic directions *in vitro*. Phenotypic profiles
256 of the isolated primary cultures are also compliant with the CD90+CD105+Vimentin+CD45-
257 CD34- profiles established for MSCs. The presence of cells positive for the CD45 and CD34
258 markers can be explained by and concomitant presence of hematopoietic cells and high
259 vascularization of the endometrial stroma in the obtained cultures, respectively. Considering a
260 precedent of the 81% CD34- and 97.5% CD34- cultures classified as CD34 negative (Lee et al.,
261 2012), we classify the obtained cultures as CD45 and CD34 negative. The percentage of cells
262 positive for CD105 seems lower than it was expected; however, literature data indicates a
263 substantial variability of this parameter for MSCs from various sources (Ponnaiyan &
264 Jegadeesan, 2014).

265 In the experiments with plasma treatment, the obtained MSCs were incubated for 24 h in the
266 control medium (the DMEM/F-12 based complete growth medium with 10% FBS) or the
267 medium supplemented with 10% PRP or 10% OP instead of FBS. We observed that under the

268 influence of PRP the cells proliferated more actively than under the influence of FBS or OP. This
269 observation indicates mitogenic effects of PRP on stromal cells. We also studied the protein
270 production levels for established markers of apoptosis and autophagy. The stress-induced protein
271 p53 is a transcription factor that regulates cell cycle and acts as a tumor suppressor
272 (Labuschagne, Zani & Vousden, 2018). An important function of p53 is to prevent the DNA
273 damage accumulation. In the case of damage to cellular DNA, p53 promotes cell cycle arrest and
274 triggers the emergency DNA repair systems; in the case of extensive DNA damage, p53 triggers
275 apoptosis (Wang, Simpson & Brown, 2015). We show that OP promotes increased production of
276 p53 protein by stromal cells, revealing a certain degree of cellular stress associated with the OP
277 treatment. At the same time, both PRP and OP have no effects on the levels of the anti-apoptotic
278 Bcl-2 protein production by MSCs. Bcl-2 is anti-apoptotic protein localized on the outer
279 mitochondrial membrane, as well as the membranes of nuclear envelope and endoplasmic
280 reticulum (Delbridge et al., 2016). Apparently, Bcl-2 activation is not involved in the effects of
281 PRP and OP.

282 We used LC3B as an autophagy marker — this protein is involved in the biogenesis of
283 autophagosomes (Barth, Glick & Macleod, 2010). Upon binding to the membrane, LC3
284 conjugates with phosphatidylethanolamine lipid (Tanida, Ueno & Kominami, 2008). After the
285 autophagosome formation, LC3-II located in the outer layer is released into the cytosol, while
286 LC3-II located in the inner layer is exposed to hydrolases. LC3B-II is conventionally used as a
287 marker of autophagosomal activity. We observed excessive production of LC3B in MSCs after
288 the exposure to PRP or OP. This observation suggests that PRP and OP contribute to self-
289 renewal of the endometrial stromal cells by enhancing autophagy.

290 Endometrial receptivity results from a combination of different characteristics of the
291 endometrium responsible for the ability to promote implantation. One of the indicators of
292 endometrial receptivity is the level of ER α , as it mediates the action of estrogens preparing the
293 endometrium for implantation by increasing its thickness via the increase in the rates of cell
294 proliferation. In clinical practice, the level of production of ER α can be evaluated by staining of
295 endometrial cells with antibodies to ER α (Glasser et al., 2002), which is expressed by several
296 subpopulations of endometrial stromal cells including MSCs (Zhou et al., 2001). We therefore
297 employed ER α as a marker reflecting the conditional receptivity of endometrium in our model.
298 We observed no significant differences in the level of ER α production upon exposure of the
299 MSCs to PRP or OP, which may indicate that the beneficial effects of these agents are estrogen-
300 independent. However, this finding should be verified on larger samples to exclude individual
301 variations in the estrogen dependence of the plasma treatment effects.

302 In addition to the susceptibility of the endometrium to the action of hormones, a certain degree of
303 its invasiveness is necessary for successful implantation. The trophoblast cells bind to the
304 endometrium, proliferate and penetrate deep into the stroma to come into contact with maternal
305 blood (Bischof, Meisser & Campana, 2000). Progressive remodeling of the extracellular matrix
306 is a hallmark of this process (Bischof, Meisser & Campana, 2002). Expression of matrix
307 metalloproteinases is observed not only in trophoblast, but also in endometrial stromal cells,
308 which provides spatial regulation of trophoblast invasion (Bischof, Meisser & Campana, 2002).

309 In our work, we took MMP9 production as an indicator of the potency of MSCs for extracellular
310 marker remodeling, an important parameter that determines the receptivity of the endometrium.
311 In our experiments, we showed that OP facilitated an increase in the MMP9 production, as
312 compared with PRP and CGM.

313 In general, the obtained results indicate stimulatory effects of PRP on endometrium in a rat
314 model, as indicated by behavior of MSCs isolated from it. Some other studies also indicate that
315 PRP enhances cell proliferation and differentiation in the uterus (Etulain et al., 2018).
316 Intrauterine administration of PRP to the rats with damaged endometrium has beneficial effects,
317 not only enhancing cell proliferation, thus promoting the tissue regeneration, but also reducing
318 fibrosis (Jang et al., 2017). The effects of OP on endometrium are notably understudied. In our
319 experiments, OP also induced the activation of autophagy in MSCs, with up-regulation of the
320 p53 and MMP9 protein expression. However, the beneficial effects of OP are less pronounced
321 and can be considered intermediate, which indicates the advantages of PRP as a treatment agent
322 for the endometrial dysfunction. This could be explained by obvious increased content of
323 mitogenic substances in platelet granules.

324 **Conclusions**

325 Mesenchymal cell cultures obtained from rat endometrium by the established protocol comply
326 with the essential criteria for multipotent stromal cells (MSCs). The treatment with platelet-rich
327 plasma (PRP) enhances proliferation of these cells with the activation of autophagy. The
328 treatment with ordinary plasma (OP) also activates autophagy with up-regulation of the stress-
329 induced protein p53 and the extracellular enzyme MMP9. Therefore, PRP could be
330 recommended as a preferable means for treating the thin endometrium. PRP usage and
331 possibilities of PRP applications in clinical practice is certainly expanding. At the same time, the
332 number of works on specific mechanisms of the PRP action on specific types of cells is
333 restricted. The establishment of molecular pathways providing cellular division after PRP
334 treatment could expand the range of PRP applications.

335 **Acknowledgements**

336 Special thanks to Natalia Usman for her help in proof-reading of the manuscript.

337

338 **References**

- 339 Aplin J. 2018. Uterus-endometrium. In: *Encyclopedia of Reproduction*. Elsevier, 326–
340 332. DOI: 10.1016/B978-0-12-801238-3.64654-8.
- 341 Arutyunyan I V., Fatkhudinov TH, El'chaninov A V., Makarov A V., Kananykhina EY,
342 Usman NY, Raimova ES, Goldshtein D V., Bol'shakova GB. 2016. Effect of
343 Endothelial Cells on Angiogenic Properties of Multipotent Stromal Cells from the
344 Umbilical Cord during Angiogenesis Modeling in the Basement Membrane Matrix.
345 *Bulletin of Experimental Biology and Medicine* 160:575–582. DOI: 10.1007/s10517-
346 016-3221-9.
- 347 Barth S, Glick D, Macleod KF. 2010. Autophagy: assays and artifacts. *The Journal of*
348 *pathology* 221:117–24. DOI: 10.1002/path.2694.
- 349 Bischof P, Meisser A, Campana A. 2000. Mechanisms of endometrial control of
350 trophoblast invasion. *Journal of reproduction and fertility. Supplement* 55:65–71.
- 351 Bischof P, Meisser A, Campana A. 2002. Control of MMP-9 expression at the maternal-
352 fetal interface. In: *Journal of Reproductive Immunology*. Elsevier, 3–10. DOI:
353 10.1016/S0165-0378(01)00142-5.
- 354 Cavallo C, Roffi A, Grigolo B, Mariani E, Pratelli L, Merli G, Kon E, Marcacci M, Filardo
355 G. 2016. Platelet-Rich Plasma: The Choice of Activation Method Affects the
356 Release of Bioactive Molecules. *BioMed Research International* 2016. DOI:
357 10.1155/2016/6591717.
- 358 Chan RWS, Gargett CE. 2006. Identification of Label-Retaining Cells in Mouse
359 Endometrium. *STEM CELLS* 24:1529–1538. DOI: 10.1634/stemcells.2005-0411.
- 360 Chan RWS, Schwab KE, Gargett CE. 2004. Clonogenicity of Human Endometrial
361 Epithelial and Stromal Cells1. *Biology of Reproduction* 70:1738–1750. DOI:
362 10.1095/biolreprod.103.024109.
- 363 Civinini R, Macera A, Nistri L, Redl B, Innocenti M. 2011. The use of autologous blood-
364 derived growth factors in bone regeneration. *Clinical Cases in Mineral and Bone*
365 *Metabolism* 8:25–31.
- 366 De Clercq K, Hennes A, Vriens J. 2017. Isolation of mouse endometrial epithelial and
367 stromal cells for in Vitro decidualization. *Journal of Visualized Experiments* 2017.
368 DOI: 10.3791/55168.
- 369 Delbridge ARD, Grabow S, Strasser A, Vaux DL. 2016. Thirty years of BCL-2:
370 Translating cell death discoveries into novel cancer therapies. *Nature Reviews*
371 *Cancer* 16:99–109. DOI: 10.1038/nrc.2015.17.
- 372 Dominici M, Le Blanc K, Mueller I, Slaper-Cortenbach I, Marini FC, Krause DS, Deans
373 RJ, Keating A, Prockop DJ, Horwitz EM. 2006. Minimal criteria for defining
374 multipotent mesenchymal stromal cells. The International Society for Cellular
375 Therapy position statement. *Cytotherapy* 8:315–317. DOI:
376 10.1080/14653240600855905.
- 377 Etulain J, Mena HA, Meiss RP, Frechtel G, Gutt S, Negrotto S, Schattner M. 2018. An
378 optimised protocol for platelet-rich plasma preparation to improve its angiogenic
379 and regenerative properties. *Scientific Reports* 8:1–15. DOI: 10.1038/s41598-018-
380 19419-6.
- 381 Glasser SR, Aplin JD, Giudice LC, Tabibzadeh S. 2002. *The endometrium*. Taylor &
382 Francis.

- 383 Jang HY, Myoung SM, Choe JM, Kim T, Cheon YP, Kim YM, Park H. 2017. Effects of
384 autologous platelet-rich plasma on regeneration of damaged endometrium in
385 female rats. *Yonsei Medical Journal* 58:1195–1203. DOI:
386 10.3349/ymj.2017.58.6.1195.
- 387 Kim H, Shin JE, Koo HS, Kwon H, Choi DH, Kim JH. 2019. Effect of autologous platelet-
388 rich plasma treatment on refractory thin endometrium during the frozen embryo
389 transfer cycle: A pilot study. *Frontiers in Endocrinology* 10. DOI:
390 10.3389/fendo.2019.00061.
- 391 Kwon A, Kim Y, Kim M, Kim J, Choi H, Jekarl DW, Lee S, Kim JM, Shin JC, Park IY.
392 2016. Tissue-specific differentiation potency of mesenchymal stromal cells from
393 perinatal tissues. *Scientific Reports*. DOI: 10.1038/srep23544.
- 394 Labuschagne CF, Zani F, Vousden KH. 2018. Control of metabolism by p53 – Cancer
395 and beyond. *Biochimica et Biophysica Acta - Reviews on Cancer* 1870:32–42. DOI:
396 10.1016/j.bbcan.2018.06.001.
- 397 Lee D-H, Sonn CH, Han S-B, Oh Y, Lee K-M, Lee S-H. 2012. Synovial fluid CD34–
398 CD44+ CD90+ mesenchymal stem cell levels are associated with the severity of
399 primary knee osteoarthritis. *Osteoarthritis and Cartilage* 20:106–109. DOI:
400 10.1016/j.joca.2011.11.010.
- 401 Lubkowska A, Dolegowska B, Banfi G. 2012. Growth factor content in PRP and their
402 applicability in medicine. *Journal of biological regulators and homeostatic agents*.
- 403 Maffulli N. 2016. *Platelet rich plasma in musculoskeletal practice*. DOI: 10.1007/978-1-
404 4471-7271-0.
- 405 Marx RE. 2019. In Situ Tissue Engineering. In: Melville J, Shum J, Young S, Wong M
406 eds. *Regenerative Strategies for Maxillary and Mandibular Reconstruction*.
407 Springer International Publishing, 73–86. DOI: 10.1007/978-3-319-93668-0_7.
- 408 Marx RE, Carlson ER, Eichstaedt RM, Schimmele SR, Strauss JE, Georgeff KR. 1998.
409 Platelet-rich plasma: Growth factor enhancement for bone grafts. *Oral Surgery,*
410 *Oral Medicine, Oral Pathology, Oral Radiology, and Endodontics*. DOI:
411 10.1016/S1079-2104(98)90029-4.
- 412 Messora MR, Nagata MJH, Furlaneto FAC, Dornelles4 RCM, Bomfim SRM, Deliberador
413 TM, Garcia VG, Bosco AF. 2011. A standardized research protocol for platelet- rich
414 plasma (PRP) preparation in rats. *RSBO Revista Sul-Brasileira de Odontologia*.
- 415 Mutlu L, Hufnagel D, Taylor HS. 2015. The Endometrium as a Source of Mesenchymal
416 Stem Cells for Regenerative Medicine1. *Biology of Reproduction* 92. DOI:
417 10.1095/biolreprod.114.126771.
- 418 Patel AN, Selzman CH, Kumpati GS, McKellar SH, Bull DA. 2016. Evaluation of
419 autologous platelet rich plasma for cardiac surgery: Outcome analysis of 2000
420 patients. *Journal of Cardiothoracic Surgery* 11. DOI: 10.1186/s13019-016-0452-9.
- 421 Pertschuk LP. 1990. *Immunocytochemistry for steroid receptors*. CRC Press.
- 422 Ponnaiyan D, Jegadeesan V. 2014. Comparison of phenotype and differentiation
423 marker gene expression profiles in human dental pulp and bone marrow
424 mesenchymal stem cells. *European Journal of Dentistry* 8:307–313. DOI:
425 10.4103/1305-7456.137631.
- 426 Tanida I, Ueno T, Kominami E. 2008. LC3 and Autophagy. In: Deretic V ed.
427 *Autophagosome and Phagosome*. Totowa, NJ: Humana Press, 77–88. DOI:
428 10.1007/978-1-59745-157-4_4.

- 429 Theoret CL, Stashak TS. 2014. Integumentary System: Wound Healing, Management,
430 and Reconstruction. In: Orsini J, Divers T eds. *Equine Emergencies*. Elsevier Inc.,
431 238–267. DOI: 10.1016/b978-1-4557-0892-5.00019-2.
- 432 Wang X, Simpson ER, Brown KA. 2015. p53: Protection against tumor growth beyond
433 effects on cell cycle and apoptosis. *Cancer Research* 75:5001–5007. DOI:
434 10.1158/0008-5472.CAN-15-0563.
- 435 Yazigi Junior JA, dos Santos JBG, Xavier BR, Fernandes M, Valente SG, Leite VM.
436 2015. Quantification of platelets obtained by different centrifugation protocols in
437 SHR rats. *Revista Brasileira de Ortopedia (English Edition)* 50:729–738. DOI:
438 10.1016/j.rboe.2015.10.008.
- 439 Yuksel EP, Sahin G, Aydin F, Senturk N, Turanli AY. 2014. Evaluation of effects of
440 platelet-rich plasma on human facial skin. *Journal of Cosmetic and Laser Therapy*
441 16:206–208. DOI: 10.3109/14764172.2014.949274.
- 442 Zhou S, Zilberman Y, Wassermann K, Bain SD, Sadovsky Y, Gazit D. 2001. Estrogen
443 modulates estrogen receptor α and β expression, osteogenic activity, and
444 apoptosis in mesenchymal stem cells (MSCs) of osteoporotic mice. *Journal of*
445 *Cellular Biochemistry* 81:144–155. DOI: 10.1002/jcb.1096.
- 446

Figure 1

Characterization of the mesenchymal cell cultures isolated from rat uterus.

A: Flow cytometry: a representative forward and side scattering dot plot with the region of interest (R1). The percentages of CD90, CD105, CD45 and CD34 positive cells in R1 are indicated. Green curve corresponds to the control (stained with secondary antibodies only).

B: Vimentin protein expression: upper image - negative control (secondary antibodies only); lower image - immunocytochemistry with anti-vimentin antibodies (red) and the nuclei counterstained with DAPI (blue). Bars, 20 μm .

C: Induced cell differentiation assay: adipogenic differentiation revealed by Sudan III staining, osteogenic differentiation revealed by alizarin red staining, and chondrogenic differentiation revealed by alcian blue staining. Upper panel - the non-induced control cells, bottom panel - cells after the induced differentiation. Bars, 50 μm .

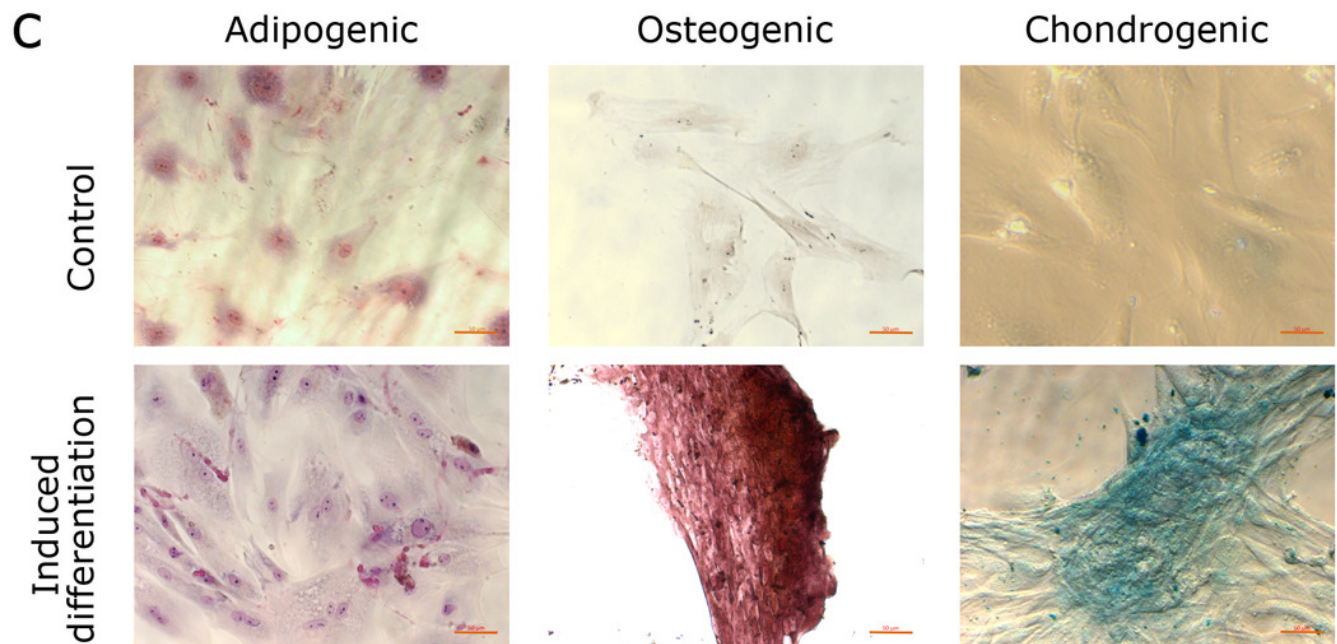
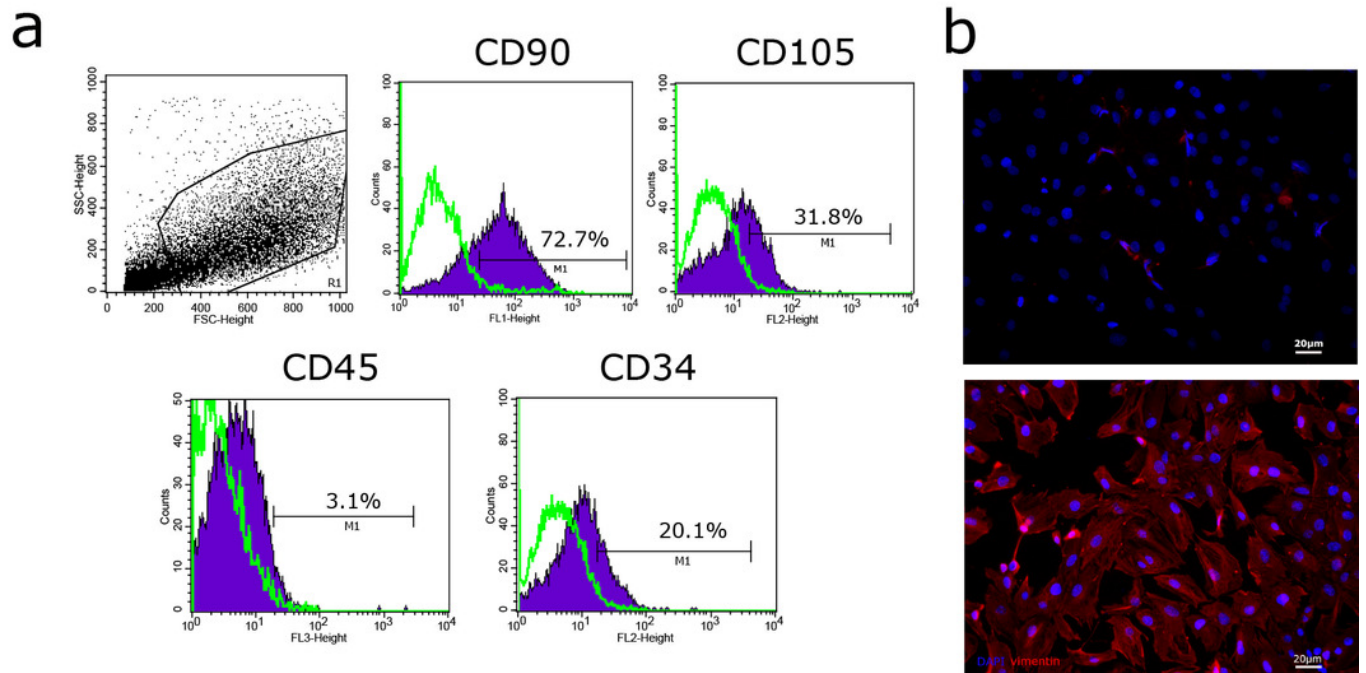


Figure 2

The assessment of cell viability and cell death after the 24 h incubation of rat uterine MSCs with complete growth medium (CGM), platelet-rich plasma (PRP), or ordinary plasma (OP).

A - immunocytochemical staining for Ki-67 (green) after 24 h exposure of the MSC cultures to the studied agents; the nuclei were counterstained with DAPI (blue). Bars, 20 μ m. B - proliferation index calculated as the number of Ki-67 positive nuclei divided by the total number of nuclei. * - $p < 0.05$ vs CGM and OP. C - a representative western blot membrane with the proteins isolated from MSCs after 24 h incubation with the studied agents, stained with p53, Bcl-2, LC3B and GAPDH specific antibodies. Relative protein levels of p53, Bcl-2 and LC3B, normalized by GAPDH level. * - $p < 0.05$ vs CGM group.

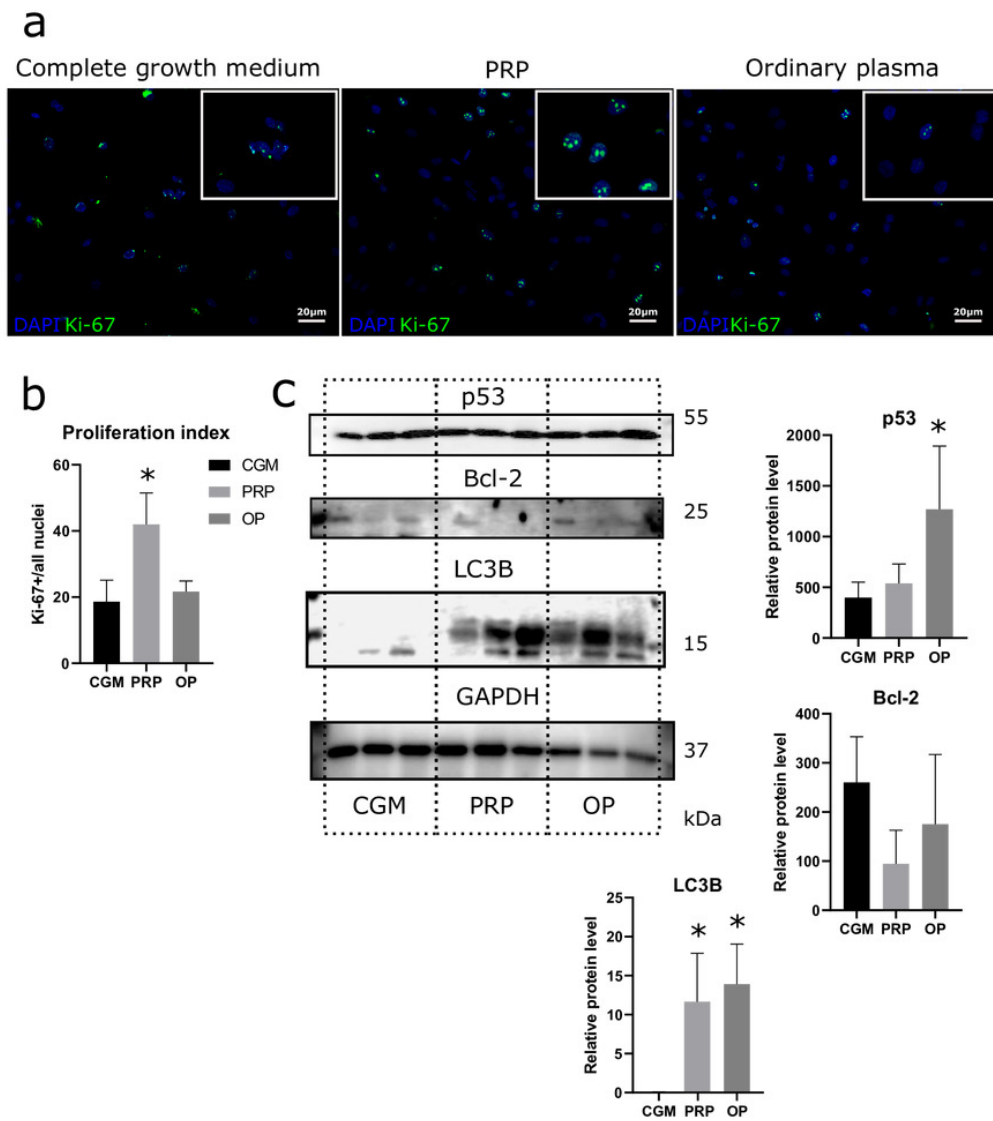


Figure 3

A representative western blot membrane with the proteins isolated from MSCs.

A representative western blot membrane with the proteins isolated from MSCs after 24 h incubation with complete growth medium (CGM), platelet-rich plasma (PRP) and ordinary plasma (OP), stained with MMP9, ER α and GAPDH specific antibodies. Relative protein levels of MMP9 and ER α , normalized by GAPDH level. * - $p < 0.05$ vs CGM group.

